

Evolution of grain structure in AA2195 Al-Li alloy plate during recrystallization

DU Yu-xuan(杜予暉), ZHANG Xin-ming(张新明), YE Ling-ying(叶凌英), LIU Sheng-dan(刘胜胆)

School of Materials Science and Engineering, Central South University, Changsha 410083, China

Received 7 June; accepted 8 October 2005

Abstract: The evolution of the grain structures in AA2195 Al-Li alloy plate warm-rolled by 80% reduction during recrystallization annealing at 500 °C was investigated by electron backscatter diffraction, scanning electron microscopy and transmission electron microscopy. It is found that the elongated grain structures are caused by the lamellar distribution of recrystallization nucleation sites, being lack of large second phase particles ($>1\ \mu\text{m}$), and dispersive coherent particles (such as δ' and β') concentrated in planar bands. The recrystallization process may be separated into three stages: firstly, recrystallization nucleation occurs heterogeneously, and the nuclei are concentrated in some planar zones parallel to rolling plane. Secondly, the grain boundaries interacted with small particles concentrate in planar bands, which is able to result in the elongated grain structures. The rate of the grain growth is controlled by the dissolution of these small particles. Thirdly, after most of small particles are dissolved, their hindrance to migration of the grain boundaries fades away, and the unrecrystallized zones are consumed by adjacent recrystallized grains. The migration of high angle grain boundaries along normal direction leads a gradual transformation from the elongated grains to the nearly equiaxed, which is driven by the tension of the grain boundaries.

Key words: AA2195 Al-Li alloy; microstructure evolution; elongated grains; equiaxed grains; recrystallization; second phase particles

1 Introduction

Aerospace and aircraft industry has a great interest in developing new aluminum alloys with high performance. AA2195 Al-Li alloy, which has high strength, very strong and rapid natural aging capability, good fracture toughness, good weldability and stress-corrosion-cracking resistance, is an ideal candidate for the application. To produce complex sheet-metal components, superplastic potential of aluminum alloys critically requires equiaxed grains with average size of less than 10 μm and high angular grain boundaries[1] which can be developed by rolling and recrystallization. AA2195 Al-Li alloy, however, is a complicated polyphase system involving in complex phase transformations. The size and shape of grains after recrystallization depend on the interaction of grain boundaries with second phase particles. Therefore, the size, distribution and morphology of the second phase particles must be carefully controlled. The aims of the

present work are to investigate the effect of the second phase precipitates on grain boundaries and recrystallization behavior in AA2195, and to find out the reason of the elongated grain structure in the alloy processed by conventional rolling routine.

2 Experimental

The AA2195 Al-Li alloy with a chemical composition of Al-3.9Cu-1.1Li-0.38Mg-0.39Ag -0.08Zr (mass fraction, %) was prepared by direct chill casting. The alloy was homogenized and hot rolled to a gauge of 10 mm. Subsequently, it was warm rolled at 350 °C by 80% reduction, followed by recrystallization annealing in a molten salt bath at 500 °C for 5 s, 30 s, 1 min, 3 min, 10 min, 30 min and 1 h to observe the evolution of the grain microstructures. The samples were quenched in water at room temperature.

EBSD examinations were carried out by means of TSL EBSD system attached to an H-3400 scanning electron microscope. For TEM examinations, the

samples were thinned to about 0.08 mm. Discs with 3 mm diameter were cut and electropolished to perforation with a twinjet polishing unit using 30% nitric acid solution in methanol at $-20\text{--}30\text{ }^{\circ}\text{C}$ and 15 V. The thin foils were examined using Tecnai G² 20 TEM at an accelerating potential of 200 kV.

3 Results

3.1 Nucleation of recrystallization

Fig.1 shows the nucleation of recrystallization in the sample annealed at $500\text{ }^{\circ}\text{C}$ for 5 s, the specimen have been sectioned in the ND-RD plane. Fig.1(a) shows the image quality (IQ) map where darker color concerns more severe distortion in lattice. Some recent investigations[2–4] also showed that the recrystallized grains and the second phase particles could be

distinguished by IQ index. As shown in Fig.1(a), the recrystallization nuclei are concentrated in the planar zones parallel to the rolling plane. For convenient analysis, 17 lamellar regions are marked out (Fig.1(b)), the second phase particles are marked black and the recrystallized grains are outlined. Obviously, most “recrystallized area” is concentrated in the 7th, 9th, 11th, 13th and 15th regions. And in the 7th, 11th and 15th regions there exist some large second phase particles which present within or beside the recrystallized area. Therefore, the conclusion may be made that the large particles serve as recrystallization nucleation sites. And this kind of regions is a bit thicker along normal direction. The 9th and 13th regions are thin and seldom large particles are found, and the recrystallized area is still aligned. Therefore, the pre-existing high angle grain boundaries must be the nucleation sites. In

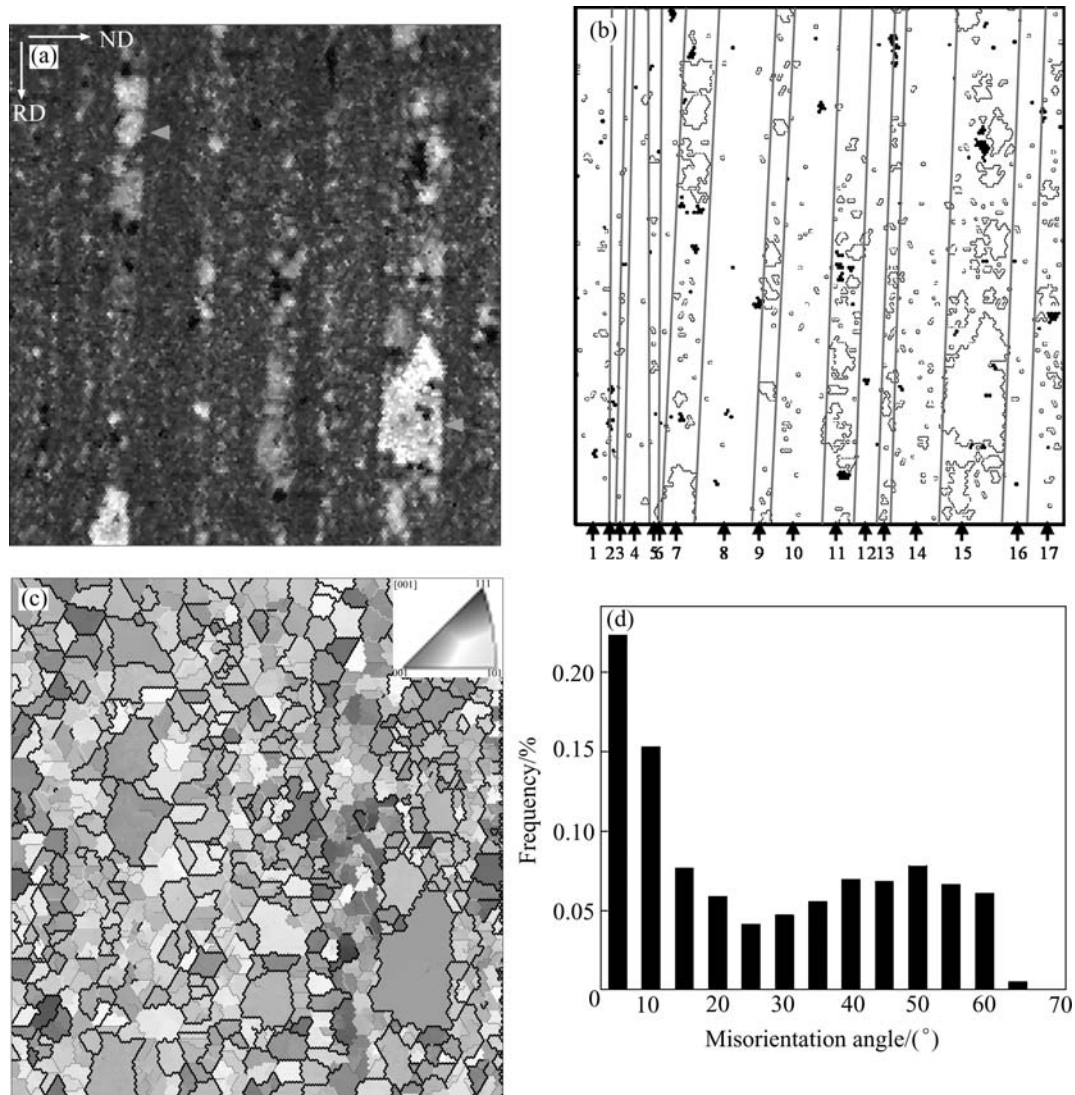


Fig.1 EBSD maps of AA2195 Al-Li alloy showing recrystallization nucleation: (a) Image quality map where darker color refers to more severe distortion in lattice; (b) Schematic diagram of recrystallization nucleation where second phase particles are marked black and some recrystallized grains are outlined; (c) Orientation map where grains are shown in Euler contrast and high angle grain boundaries as black lines; (d) Distribution of boundary misorientations

Figs.1(a) and (b), some areas remain totally unrecrystallized, e.g. the 4th, 8th and 12th regions, in which nucleation might be inhibited, or recrystallization proceeds rather slowly. In addition, some straight boundaries (marked by arrows in Fig.1(a)) parallel to rolling plane show there exists something restraining the migration of grain boundaries in ND.

From the orientation map(Fig.1)), it is found that the orientations of the recrystallized grains are random orientations instead of cube orientation which is typical recrystallization crystallographic orientation in fcc metals[5]. This also implies particle stimulated nucleation(PSN) happening in heavily deformed polycrystals[6, 7], which leads to a random texture. It can be seen from Fig.1(d) that the unrecrystallized area mentioned above is still a deformation structure or recovery structure with low misorientation and subgrains. The large amount of low angle boundaries in Fig.1(d) indicates that recrystallization just starts.

3.2 Development of lamellar structure

Fig.2 shows the development of the elongated grain structure during annealing. At 500 °C only for 30 s, large

amount of the recrystallized areas presented in Fig.2(a) shows that the recrystallization in the sample is a rapid process. However, there still exist some band-like areas with high lattice distortion that are stable even after annealing for 10 min(Fig.2(b)). It is also observed that a few thin recrystallized-like bands exist inside the unrecrystallized areas. The emergence of such bands, which should be the result of new recrystallization, leads the unrecrystallized areas to be split into the thinner gradually. After 30 min, the fraction of the recrystallized areas increases obviously and almost reaches 95% after 1 h(Figs.2(c), (d) and Fig.3).

On the other hand, the lamellar grain structure forms just at the beginning of annealing. It seems that there are some obstacles to the migration of the grain boundaries in ND, which separates the sample into the planar bands, and the recrystallized grains can grow only inside the bands. In the thick bands, the nucleation sites seem to be spread, and the grains with various sizes are developed. The grain aspect ratio (d_{RD}/d_{ND}), defined as the ratio of the grain boundaries intercept lengths in the rolling direction to those in the normal direction, is relatively low. Whereas, in the thin bands, the line

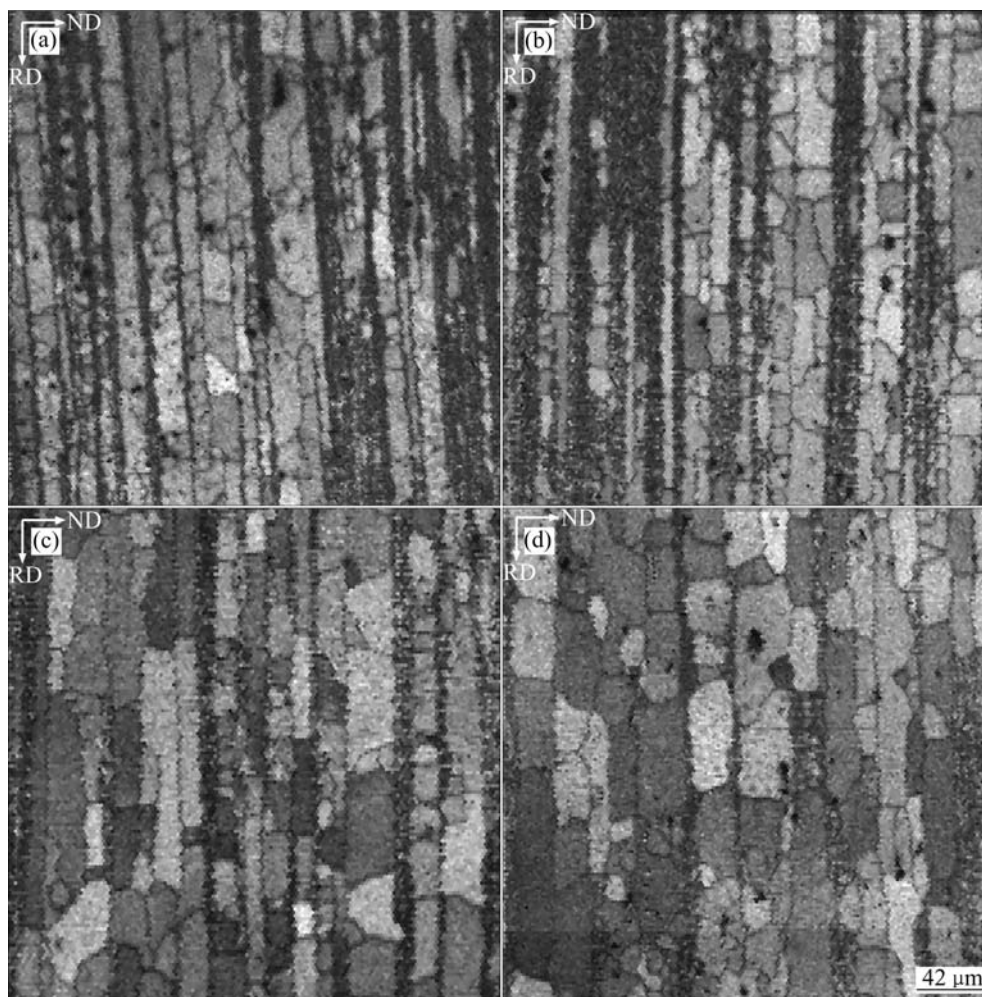


Fig.2 IQ maps of AA2195 specimen annealed at 500 °C for 30 s(a), 10 min(b), 30 min(c) and 1 h(d)

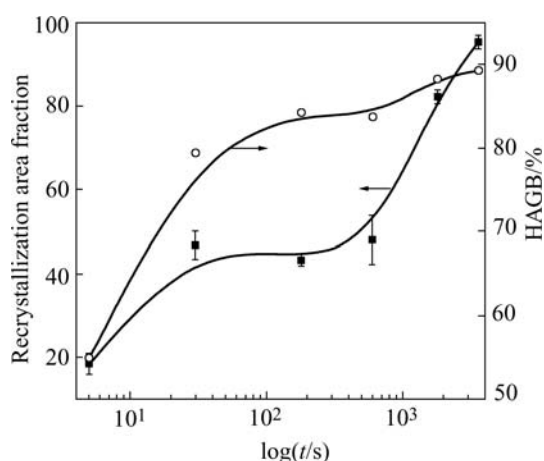


Fig.3 Recrystallization area fraction and high angle boundaries (HAGB) as function of annealing time

density of the nucleation sites is low in RD, just pancake grains of large d_{RD}/d_{ND} are found. After 30 min, the large grains consume small ones and grow up especially in the thick bands, which results in the change of the grain shape into a thick pancake. As shown in Fig.2(c), d_{ND} increases. Some thin grains would be consumed by other larger ones because they have no size advantage. After 1 h, the grains transform to equiaxial due to large surface energy of the pancake grains. Fig.4 shows the clear coarsening process of the grains. The size of the recrystallized grains increase rapidly to 6.4 μm after 30 s. Then, the recrystallization does not speed up till annealing for about 10 min. However, after 30 min, the grains grow significantly.

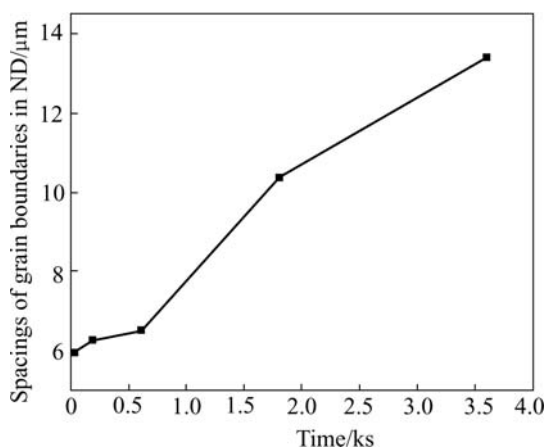


Fig.4 Spacing of grain boundaries in ND as function of annealing time

3.3 Evolution of second phase particles during annealing

Fig.5(a) shows the distribution and morphology of the second phase particles in the as-rolled sample, including not only a large amount of small particles, but

only a few large ones ($>1 \mu\text{m}$). The particles distribute so non-uniformly that some concentrated in the regions which are marked with the dash box in Fig.5(a), and others are aligned with the rolling plane (marked by arrows). Whereas, after annealing for 1h, a large amount of small particles are dissolved, and only some coarsened particles are found as shown in Fig.5(b).

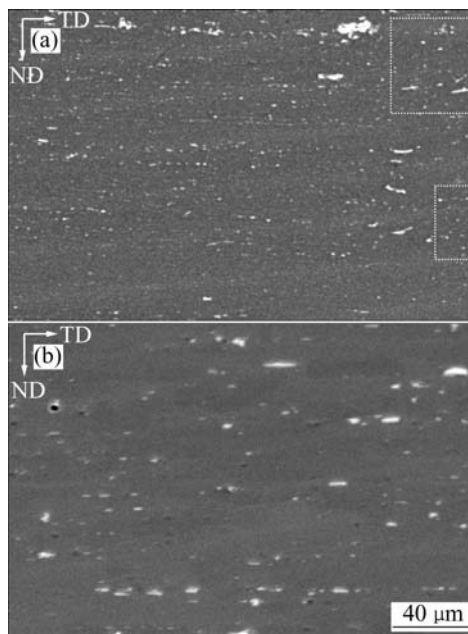


Fig.5 SEM backscattered electron images of AA2195 sample: (a) As-rolled; (b) Annealed at 500 $^{\circ}\text{C}$ for 1 h

In TEM examinations, smaller coherent particles including δ' (Al_3Li) and β' (Al_3Zr) are found in Figs.6 and 7 (dark spherical particles). Most of the grains with rather low dislocation density, i.e. recrystallized grains, are concentrated around large particles as shown in Fig.6(b). And small particles, including both small (about 20 nm) and relatively large (about 0.1 μm) particles, restrain the migration of high angle boundaries as shown in Fig.7.

4 Discussion

4.1 Effect of second phase particles

In the AA2195 Al-Li alloy specimen, the addition of trace Ag and Mg makes the precipitation more complicated [10]. SALEM et al[11] found that in as-rolled Al-Cu-Li alloys (AA2095 and AA2195), the coarse second phase including δ (AlLi), θ' (Al_2Cu), T_1 (Al_2CuLi), T_2 (Al_6CuLi), T_B ($\text{Al}_{15}\text{Cu}_8\text{Li}_2$), S' (Al_2CuMg) present within the grains, and mostly at the grain boundaries and triple points. During hot-rolling, many phases, including those with sizes below 1 μm , precipitate at the grain boundaries, which are aligned with rolling plane because most grains are elongated

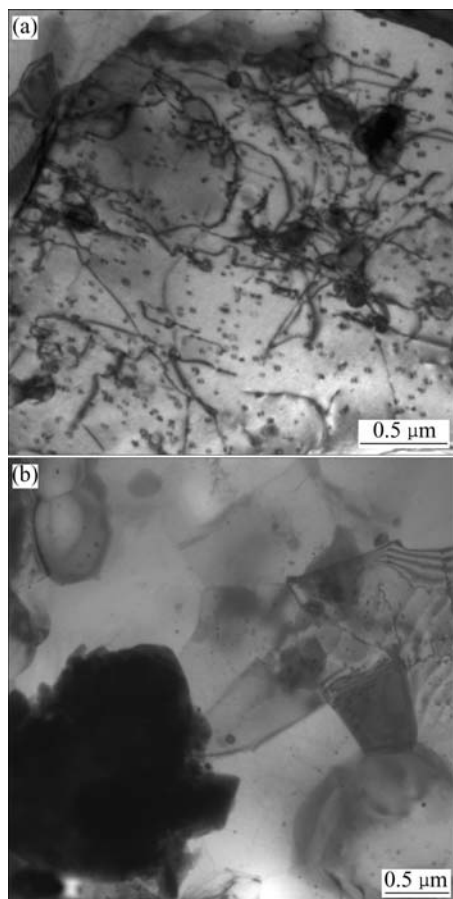


Fig.6 TEM micrographs showing distribution of second phase particles(a) and recrystallization around large particles(b)

during rolling process, i.e. the particles are to be aligned at the pre-existing boundaries as shown in the arrow regions in Fig.5(a). According to SUZUKI et al[12], small coherent β' particles will be present in layered distribution. And small coherent δ' particles often precipitate around β' precipitates[13]. They may also concentrate in planar bands. So the coarse particles, β' and δ' precipitates constitute the “obstacles” to migration of the grain boundaries. Fig.7 shows the evidence of these particles restraining migration of the grain boundaries.

It is well known that the large particles could serve as recrystallization positions due to inhomogeneous deformation around them, which leads to high misorientation gradient and dislocation density. JAZAERI and HUMPHREYS[14,15] found that the large particles were helpful to the break-up of lamellar grain microstructure and production of high angle boundaries and decreased the grain aspect ratio near large particles during deformation that benefited the recrystallization.

On the other hand, small particles strongly hinder the migration of GB, and, therefore, they suppress recrystallization. In the present study, small particles were inhomogeneous distributed, e.g. the ones concentrated in

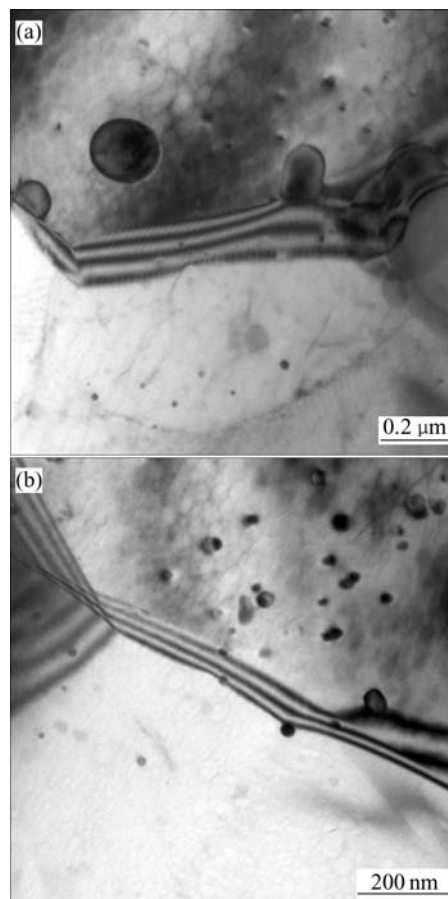


Fig.7 TEM micrographs of second phase particles at medium(a) and small size pinning grain boundaries(b) during annealing at 500 °C

some regions and the ones in planar band parallel to rolling plane, which leads to stagnancy of recrystallization in some regions and migration of grain boundaries in ND, respectively. Some unrecrystallized or recovered regions were presented between the recrystallized ones. This is proved by the stable unrecrystallized or recovery regions and lamellar grain structure in Fig.1(a) and Fig.2. However, after the small particles have been dissolved gradually, these regions have no advantage of size or orientation to the growth, and would be consumed by existing large recrystallized grains. Therefore, they have no significant effect on changing lamellar structure.

4.2 Evolution of recrystallization structure

From the above discussion, the nucleation sites might include deformation zones close to large particles or some pre-existing high angle grain boundaries. In a rolled and elongated grain structures, most pre-existing grain boundaries are parallel to rolling plane. And rolling, which is a near plane strain compression, and characteristics of deformation zones close to large particles led nucleation sites to be aligned with rolling plane. As shown in Fig.1(a), the nuclei are inhomogeneously distributed due to lack of enough large

particles and orientation pinning in deformed matrix. The migration rate of nuclei originated in the region close to the large particles is high, while nucleation or some recovery process is presented in deformed matrix, but the misorientation and mobility of grain boundaries are low. Therefore, the real nucleation rate is low, which is one of the reasons of the large final grain size.

As shown in Fig.2, the fraction of recrystallized area rapidly reaches 80% after annealing for 30 s, but it keeps stable in succession. In some regions, for the reason of small particles concentrating there, recrystallization seems to be stagnated until annealing for beyond 10 min (Fig.2). During this period, some planar recrystallized regions present inside these unrecrystallized regions and become thicker gradually with process of annealing. Actually, this process is very slow so that the size in ND is much smaller than that in the other regions, and these regions might have higher dislocation density because only recovery process should appear, which results that they would be consumed after entirely dissolving of particles pinning grain boundaries due to their higher energy and small size. On the other hand, in the recrystallized regions, because of the planar distribution of small particles and recrystallization nuclei as described above, the grains appear a shape of pancake. In some regions lack of nuclei, the grain aspect ratio is very large. While dissolving of the small particles, high surface tension of pancake grains drive them to be nearly equiaxed slowly. As shown in Fig.2(c), the grain size in ND increased significantly, and the grain aspect ratio decreased after annealing for 30 min.

5 Conclusions

1) The lamellar grain structure occurs because of lamellar distribution of recrystallization nucleation sites such as pre-existing high angle grain boundaries and highly misoriented deformation zones around large particles, lack of large second phase particles ($>1\ \mu\text{m}$) and dispersive coherent particles (such as δ' and β') are concentrated in the planar bands.

2) Recrystallization process of the warm rolled AA2195 Al-Li plate may be separated into three stages: firstly, recrystallization nucleation occurs heterogeneously, and the nuclei concentrates in some planar zones parallel to rolling plane; secondly, the grain boundaries interact with small particles concentrated in planar bands, which is able to result in the elongated grain structures. The rate of the grain growth is controlled by the dissolution of these small particles. Thirdly, after most of small particles are dissolved, their hindrance to migration of the grain boundaries fades

away, and the unrecrystallized zones are consumed by adjacent recrystallized grains. And the migration of high angle grain boundaries along ND (normal direction) leads a gradual transformation from the elongated grains to the nearly equiaxed, which is driven by the tension of the grain boundaries.

Acknowledgements

The authors would like to acknowledge Mr. YANG Xu-yue and the University of Electro-communications for determining the EBSD data and analysis.

References

- [1] NIEH T G, WADSWORTH J, SHERBY O D. Superplasticity in Metals and Ceramics[M]. Cambridge: Cambridge University Press, 1997. 1–90.
- [2] BLACK M P, HIGGINSON R L. An investigation into the use of electron back scattered diffraction to measure recrystallised fraction[J]. Scripta Materialia, 1999, 41(2): 125–129.
- [3] TARASIUK J, GERBER P, BACROIX B. Estimation of recrystallised volume fraction from EBSD data[J]. Acta Materialia, 2002, 50: 1467–1477.
- [4] WILSON A W, MADISON J D, SPANOS G. Determining phase volume fraction in steels by electron backscattered diffraction[J]. Scripta Materialia, 2001, 45: 1335–1340.
- [5] GOTTSTEIN G. Evolution of recrystallization textures—classical approaches and recent advances[A]. Proceedings of the 13th International Conference on Textures of Materials[C]. Switzerland: Trans Tech Publications Ltd., 2002. 1–24.
- [6] HUMPHREYS F J, HATHERLY M. Recrystallization and related annealing phenomena[J]. Great British: Pergamon, 1995. 235–280.
- [7] DOHERTY R D, HUGHES D A, HUMPHREYS F J, et al. Current issue in recrystallization: a review[J]. Mater Sci Eng A, 1997, A238: 219–274.
- [8] WESTWOOD A R C. New materials for aerospace industry[J]. Mater Sci Tech, 1990, 6: 958–961.
- [9] PICKENS J R, HEUBAUM F H, LANGAN T J, KRAMER L S. Al-(4.5-6.3)Cu-1.3Li-0.4Ag-0.4Mg-0.14Zr alloy weldalite™ 049[A]. Proceedings of the fifth International Aluminum-Lithium Conference[C]. Virginia: Williamsburg, 1989. 1397–1414.
- [10] HUANG B P, ZHENG Z Q. Independent and combined roles of trace Mg and Ag additions in properties precipitation process and precipitation kinetics of Al-Cu-Li-(Mg)-(Ag)-Zr-Ti alloys[J]. Acta Materialia, 1998, 46(12): 4381–4393.
- [11] SALEM H G, GOFOSTH R E, HARTWIG K T. Influence of intense plastic straining on grain refinement, precipitation and mechanical properties of Al-Cu-Li-Based alloys[J]. Metall Mater Trans A, 2003, 34A: 1153–1161.
- [12] SUZUKI H, KANNO M, SAITOH H. Different effects between Zr and Cr additions on recrystallization of hot-rolled Al-Zn-Mg-Cu alloys[J]. Journal of Japan Institute of Light Metals, 1986, 36(1): 22–28.
- [13] KUMAR K S, BROWN S A, PICKENS J R. Microstructural evolution during aging of an Al-Cu-Li-Ag-Mg-Zr alloy[J]. Acta Materialia, 1996, 44(5): 1899–1915.
- [14] JAZAERI H, HUMPHREYS F J. The transition from discontinuous to continuous recrystallization in some aluminium alloys I—the deformed state[J]. Acta Materialia, 2004, 52: 3239–3250.
- [15] JAZAERI H, HUMPHREYS F J. The transition from discontinuous to continuous recrystallization in some aluminium alloys II—annealing behavior[J]. Acta Materialia, 2004, 52: 3251–3262.

(Edited by LONG Huai-zhong)